

Theoretical Study of Hypervalent Bonds in 1,6-Diaza-1,6-dihydro- and 1,6-Dihydro-1,6-dioxapentalene Systems with a Heteroatom X at 6a Position (X = 14–16 Group Atoms)

Teruo Atsumi,[1] Tomohiro Abe,[1] Kin-ya Akiba,[2] and Hiromi Nakai*[1,2]

[1]Department of Chemistry and Biochemistry, School of Advanced Science and Engineering, Waseda University, Tokyo 169-8555

[2]Research Institute for Science and Engineering, Waseda University, Tokyo 169-8555

Received February 1, 2010; E-mail: nakai@waseda.jp

The present study theoretically investigated hypervalent bonding systems with the skeleton of pentalene. Geometries and energetics were examined by density functional theory calculations with triple-zeta class basis sets. The bond energies of the O–X and N–X hypervalent three-center four-electron bonds were estimated. Furthermore, the relationships between the bond-switching equilibration reactions and the stabilities of the hypervalent bonding intermediates were examined.

Experimental studies of the bond-switching equilibration of 5-(1-aminoethylidene)amino-3-methyl-1,2,4-thiadiazole (**1**) and 5-(2-amino-1-propenyl)-3-methylisothiazole (**2**) systems with nitrogen-15 isotope, as shown in Scheme 1, have been reported.[1–6] An intermediate B_{sym}, which is symmetric and has 10-S-3 sulfurane (three coordinate hypervalent sulfurane bearing two equatorial lone pair electrons) consisting of a hypervalent three-center four-electron (3c-4e) bond in N–S–N, was invoked to realize the equilibrium between A(α) and A(β).

As derivatives of **2**, 1,6-dihydro-1,6-dioxa-6a-thiapentalene (**2′**) systems were also synthesized as stable compounds, which have symmetric geometries, B_{sym}, and 10-S-3 sulfurane consisting of 3c-4e bond in O–S–O (Chart 1).[7,8]

On the other hand, the bond-switching equilibration cannot be found for the corresponding oxygen analogs, i.e., 1,2,4-oxadiazole **3** and isoxazole **4** systems in Scheme 2.[6] The differences between **1** and **3** and between **2** and **4** are only the central atoms.

Our previous study[9] theoretically investigated the reaction mechanism for the bond-switching equilibration on sulfur **14** and oxygen **13**, employing the simplified models as shown in Scheme 3. In this model, the pathway from A(α) to B_{sym} is the same as from A(β) to B_{sym}, because of the symmetry. Geometries and energetics of the reactants, products, and intermediates were examined along unimolecular and bimo-

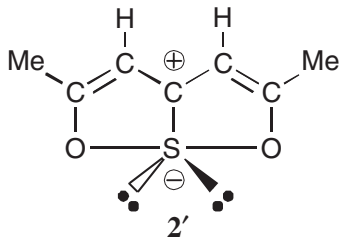

Chart 1. Compound **2′**.

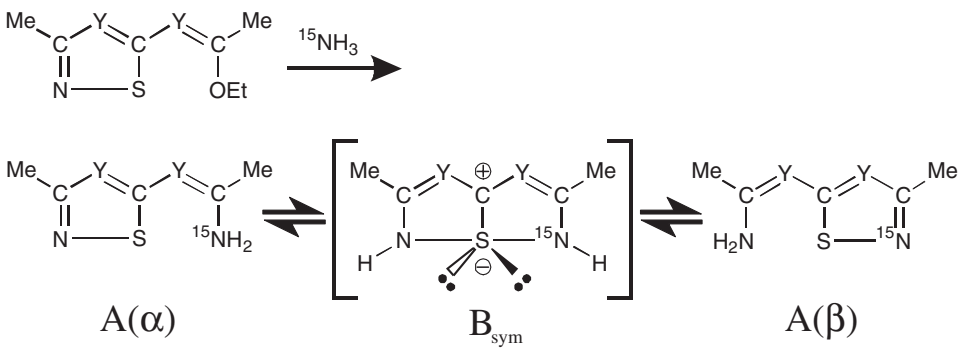

Scheme 1. Bond-switching equilibration of 5-(1-aminoethylidene)amino-3-methyl-1,2,4-thiadiazole (**1**) and 5-(2-amino-1-propenyl)-isothiazole (**2**).

Published on the web July 24, 2010; doi:10.1246/bcsj.20100027

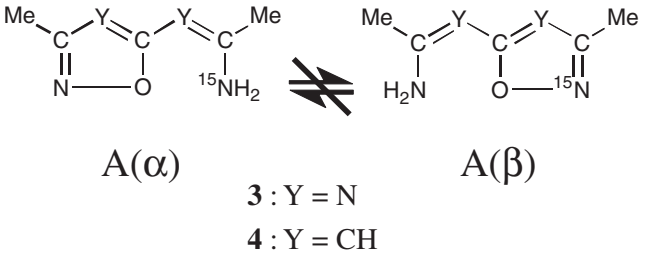

Scheme 2. Bond-switching equilibration of 1,2,4-oxadiazole **3** and isoxazole **4**.

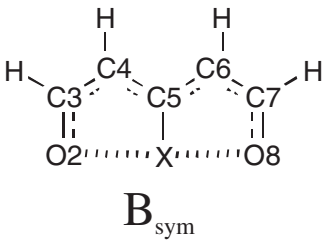

5′–8′: X = CH_2, SiH_2, GeH_2, SnH_2
9′–12′: X = NH, PH, AsH, SbH
13′–16′: X = O, S, Se, Te

Chart 2. Compounds **5′–16′**.

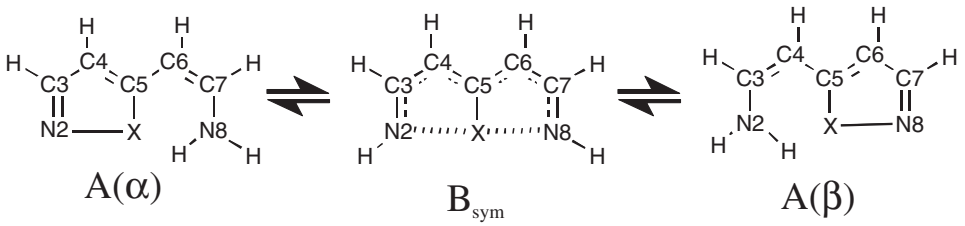

5–8: X = CH_2, SiH_2, GeH_2, SnH_2
9–12: X = NH, PH, AsH, SbH
13–16: X = O, S, Se, Te

Scheme 3. Bond-switching equilibration of **5–16**.

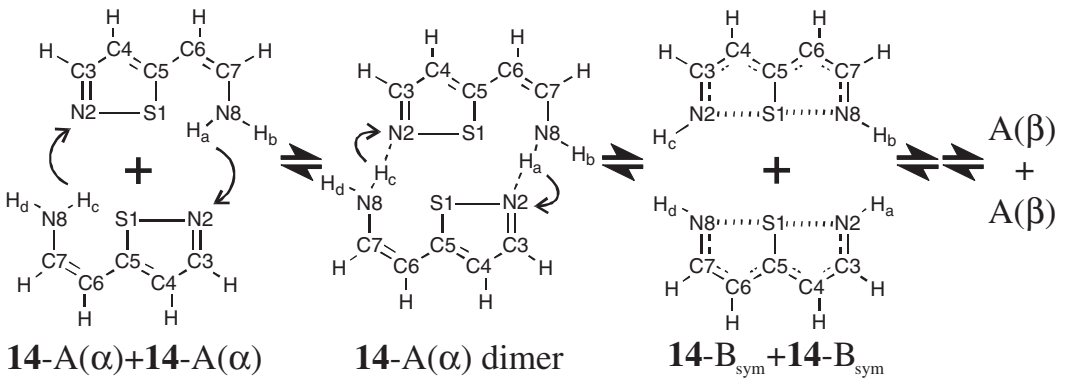

14-A(α)+**14**-A(α) **14**-A(α) dimer **14**-B_{sym}+**14**-B_{sym}

Scheme 4. Bimolecular reaction of **14**.

lecular reaction paths by density functional theory (DFT) calculations by taking into account solvent effects. Furthermore, the transition states (TSs) and the intrinsic reaction coordinates were investigated. The unimolecular reaction path had high energy barriers around 70 kcal mol^{-1} (1 kcal mol^{-1} = 4.184 kJ mol^{-1}) in **13** and **14**. It was concluded that the unimolecular bond-switching reactions cannot proceed thermally, and the solvent effect leads to minor change.

In the bimolecular processes as shown in Scheme 4, the bond-switching reaction of **14** with X = S could be accomplished with the energy barrier of about 40 kcal mol^{-1}. On the other hand, that of **13** with X = O could not occur even in the bimolecular processes, because **13**-B_{sym} was obtained as a TS which leads to a high energy barrier of about 70 kcal mol^{-1}. As a result, the stability of B_{sym} plays a key role for the bond-switching equilibration reaction.

The aim of this theoretical study is to clarify the stability of hypervalent compounds B_{sym} for a wide variety of central atoms, group 14–16 and period 2–5 elements, **5–16** in Scheme 3 and **5′–16′** in Chart 2, and estimate hypervalent bond energies of them. The compounds of numbers with prime are produced from corresponding nitrogen analogs in Scheme 3 by replacing NH with O at positions 2 and 8. The reason the pentalene systems were adopted as models is as follows. The bond energy of a hypervalent N–S bond was estimated to be around 16.6 kcal mol^{-1} experimentally by employing 1,6-dihydro-6a-thia-1,6-diazapentalene fused with two pyrimidine rings.[10] Recent theoretical study of the same system found the corresponding energy to be 15.7 kcal mol^{-1}.[11] Therefore, we here adopted the 1,6-diaza-1,6-dihydro- and 1,6-dihydro-1,6-dioxapentalene systems with a heteroatom X at 6a position for theoretical estimation of hypervalent bond energy of O–X and

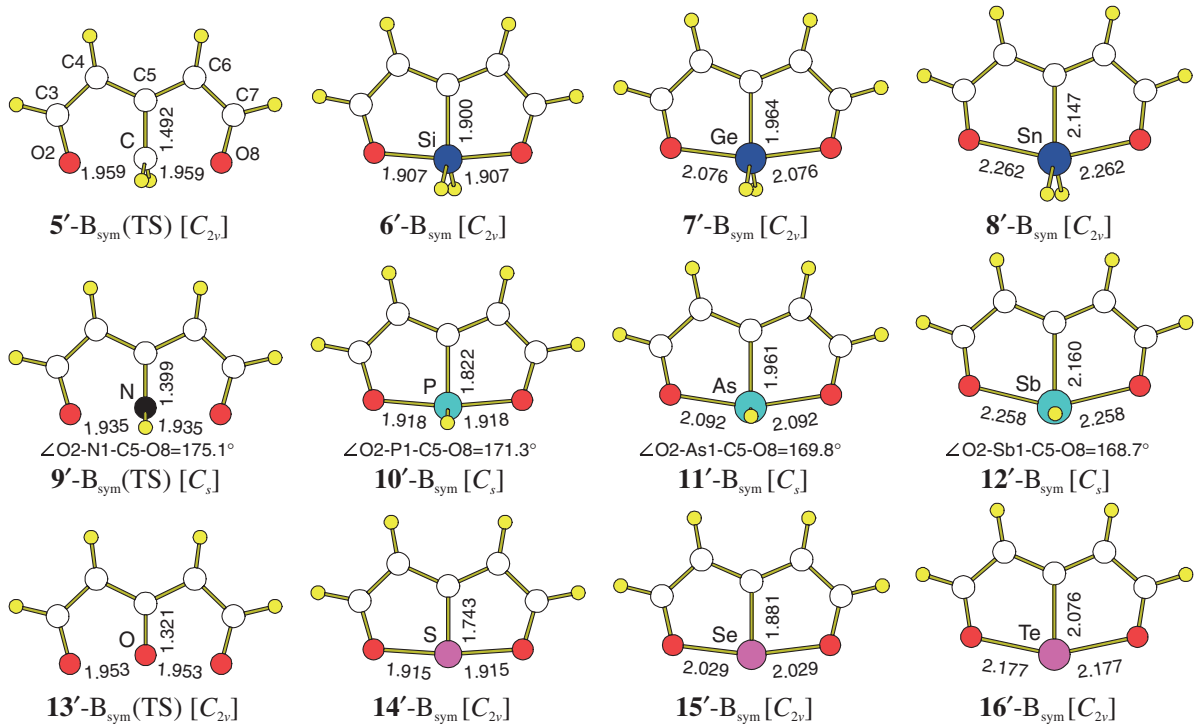

Figure 1. Geometries of B_{sym} of **5′–16′** (in Å).

N–X of a variety of main group elements (X). The discussion of the hypervalent bond based on the results is restricted to these systems. However, we expect at present that the results are worthy as a first-step effort for comparing the hypervalent bonds with a wide variety of central atoms, group 14–16 and period 2–5 elements, which will motivate not only theoretical but also experimental studies.

The organization of the present paper is as follows. The second section presents the computational methods adopted in this study. The third section describes the results and discussion, which involves the geometric structures, energies, and estimation of hypervalent bond energies of B_{sym} in **5′–16′** and in **5–16**, and the bond-switching reactions of **5–16**. Concluding remarks are summarized in the last section.

Computational Method

The present study theoretically examined the compounds **5–16** in Scheme 3 and their oxygen analogs **5′–16′** in Chart 2. The geometries were optimized by DFT calculations with the B3LYP hybrid functional,[12] which consists of the Hartree–Fock exchange, the Slater exchange,[13] the Becke (B88) exchange,[14] the Vosko–Wilk–Nusair (VWN5) correlation,[15] and the Lee–Yang–Parr (LYP) correlation[16] functionals. The correlation consistent polarization plus valence triple zeta (cc-pVTZ) basis sets of Dunning[17,18] for atoms of period 1–4 elements, and cc-pVTZ with small-core relativistic pseudopotentials (cc-pVTZ-pp)[19] for atoms of period 5 elements were adopted. Geometry optimizations of B_{sym} were performed maintaining a C_s or C_2 symmetry. Frequency analyses were performed in order to check the stable geometry with no imaginary frequencies or the TS with one imaginary frequency. The above first-principle calculations were carried out with the Gaussian 03 suite of programs.[20] Since the previous study[9] of **13** and **14** showed that solvent effect is minor matter in energy for the stability of B_{sym} as well as A, the present calculations do not include the effect.

Results and Discussion

O–X–O Hypervalent Bonds. This section shows the theoretical investigation of geometries and energies of B_{sym} of **5′–16′** in Chart 2 and the estimation of the O–X–O hypervalent bond energies. Figure 1 shows the geometries of B_{sym}. In each system, the bond length of X1–O2 is equal to that of X1–O8 because of fixing the C_s or C_2 symmetry. For the cases of groups 14 and 16, the species of B_{sym} had C_{2v} symmetry, i.e., dihedral angle ∠O2–X1–C5–O8 was equal to 180° and the pentalene skeleton was planar. For the cases of group 15, the species of B_{sym} had C_s symmetry with 168.7–175.1° of ∠O2–X1–C5–O8, which were approximately in plane. The compounds with the central atoms X1 of period 3–5 elements were obtained as stable structures. On the other hand, B_{sym} with the central atoms X1 of period 2 elements were obtained as TSs: i.e., **5′**-B_{sym}, **9′**-B_{sym}, and **13′**-B_{sym}. The bond lengths of C5–X1 increase with higher period elements of the same group: for example, 1.492, 1.900, 1.964, and 2.147 Å for [**5′**: CH_2], [**6′**: SiH_2], [**7′**: GeH_2], and [**8′**: SnH_2], respectively. This trend is because of the increase of the atomic radius for higher period elements. The bond lengths of X1–O2 and X1–O8 also show a similar trend except for the relationships between periods 2 and 3. For example, 1.959 Å for [**5′**: CH_2] is longer than 1.907 Å for [**6′**: SiH_2]. This inversion might be related to the strength of the O–X–O hypervalent bond.

Next, we estimated bond energies of the hypervalent O–X–O bonds in B_{sym} by investigating two processes to cleave the X1–O8 bonds, namely, rotation of C5–C6 or C6–C7 bond, giving B′(α) or B″(α), respectively, as shown in Scheme 5.

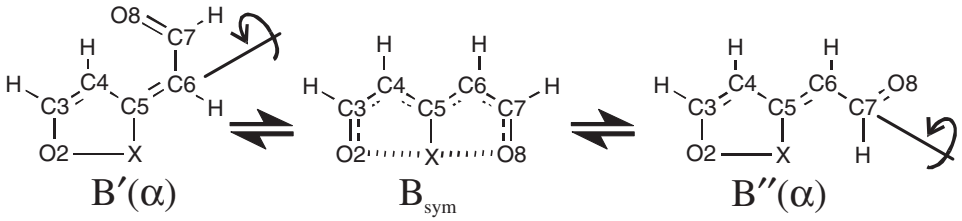

Scheme 5. Rotations of C5–C6 and C6–C7 bonds of **5′–16′** systems.

Table 1. O–X Bond Length in HOXH and **5′–16′** (in Å)[a]

	5′	**6′**	**7′**	**8′**	**9′**	**10′**	**11′**	**12′**	**13′**	**14′**	**15′**	**16′**
X	CH_2	SiH_2	GeH_2	SnH_2	NH	PH	AsH	SbH	O	S	Se	Te
Group	14	14	14	14	15	15	15	15	16	16	16	16
Period	2	3	4	5	2	3	4	5	2	3	4	5
HOXH	1.420	1.660	1.792	1.993	1.447	1.673	1.816	1.999	1.452	1.683	1.820	1.993
B′	1.449	1.707	1.850	2.063	1.424	1.707	1.859	2.051	1.451	1.696	1.841	2.024
	(0.029)	(0.047)	(0.058)	(0.070)	(−0.023)	(0.034)	(0.043)	(0.052)	(−0.001)	(0.013)	(0.021)	(0.031)
B″	1.473	1.711	1.857	2.075	1.432	1.713	1.869	2.063	1.433	1.710	1.861	2.053
	(0.053)	(0.051)	(0.065)	(0.082)	(−0.015)	(0.040)	(0.053)	(0.064)	(−0.019)	(0.027)	(0.041)	(0.060)
Exptl[b]	1.43	1.66	1.65	1.95	1.46	1.63	1.78	2.00	1.48	1.50	1.61	2.00
	(0.01)	(−0.00)	(−0.14)	(−0.04)	(0.01)	(−0.04)	(−0.04)	(0.00)	(0.03)	(−0.18)	(−0.21)	(0.01)

a) The deviations from the HOXH case are shown in parentheses. b) Ref. 21.

Table 2. Energetics for **5′–16′** (in kcal mol^{-1})

	5′	**6′**	**7′**	**8′**	**9′**	**10′**	**11′**	**12′**	**13′**	**14′**	**15′**	**16′**
X	CH_2	SiH_2	GeH_2	SnH_2	NH	PH	AsH	SbH	O	S	Se	Te
Group	14	14	14	14	15	15	15	15	16	16	16	16
Period	2	3	4	5	2	3	4	5	2	3	4	5
ΔE(B′)	−19.25	15.50	15.06	19.71	−17.93	13.41	15.49	19.87	−13.00	17.23	23.68	29.52
ΔE(B″)	−18.70	13.43	12.56	15.95	−15.41	12.87	14.00	16.96	−10.01	18.18	23.11	26.98
$\overline{\Delta E}$	−18.98	14.47	13.81	17.83	−16.67	13.14	14.75	18.42	−11.50	17.71	23.39	28.25
E_{CB}(O–X)[a]	93.78	120.30	100.04	88.35	66.52	87.58	77.73	74.66	52.35	68.55	64.48	63.80
	(85.56)	(108.22)	(86.72)	(133.06)	(47.80)	(97.23)	(71.91)	(75.01)	(33.89)	(63.31)	(81.94)	(64.02)
E_{HB}(O–X–O)	74.81	134.77	113.85	106.19	49.85	100.72	92.47	93.07	40.85	86.26	87.87	92.05
E_{HB}(O–X)	37.40	67.38	56.93	53.09	24.93	50.36	46.24	46.54	20.43	43.13	43.94	46.02

a) Experimental values given in parentheses are taken from Ref. 21.

These processes involve the change of the character of X1–O2 bond from a hypervalent bond to a normal covalent bond in addition to the cleavage of the X1–O8 hypervalent bond.

Consequently, the energy difference between B′ and B$_{sym}$ or between B″ and B$_{sym}$, ΔE(B′) or ΔE(B″), is approximately equivalent to the difference between the O–X–O hypervalent bond energy, E_{HB}(O–X–O) (=$2E_{HB}$(O–X)) and the O–X covalent bond energy, E_{CB}(O–X):

$$\Delta E(B') \approx \Delta E(B'') \approx E_{HB}(O–X–O) - E_{CB}(O–X) = 2E_{HB}(O–X) - E_{CB}(O–X) \quad (1)$$

In order to estimate E_{CB}(O–X), we calculated HOXH, HO•, and •XH molecules at the same level:

$$E_{CB}(O–X) \approx E(HO•) + E(•XH) - E(HOXH) \quad (2)$$

The approximate estimations of E_{HB}(O–X–O) and E_{HB}(O–X) by eqs 1 and 2 postulate that the covalent bond energies of O–X in HOXH are close to those in B′ and B″, in which the O–X bond is contained in a five member ring, X1–O2–C3–C4–C5. Table 1 compares the O–X bond lengths in B′, B″, and HOXH.

We compared the calculated O–X covalent bond lengths with experimental values in order to check the reliability of theoretical treatment in this study. The deviations from the HOXH case, which are shown in parentheses in Table 1, are less than 0.082 Å. In Table 1, the experimental O–X covalent bond lengths are also listed.[21] Deviations of experiments are smaller than 0.04 Å, except for 0.14, 0.18, and 0.21 Å for Ge, S, and Se, respectively, because of the existence of double-bond character in the experiment.

Table 2 shows the relative energies of B′ and B″, ΔE(B′) and ΔE(B″), their average values, $\overline{\Delta E}$ (=(ΔE(B′) + ΔE(B″))/2), and estimated bond energies, E_{CB}(O–X), E_{HB}(O–X–O), and E_{HB}(O–X), for **5′–16′**. The estimations of E_{HB}(O–X–O) and E_{HB}(O–X) in Table 2 adopted the average value $\overline{\Delta E}$:

$$E_{HB}(O–X–O) = E_{CB}(O–X) + \overline{\Delta E} \quad (3)$$

$$E_{HB}(O–X) = \frac{1}{2}(E_{CB}(O–X) + \overline{\Delta E}) \quad (4)$$

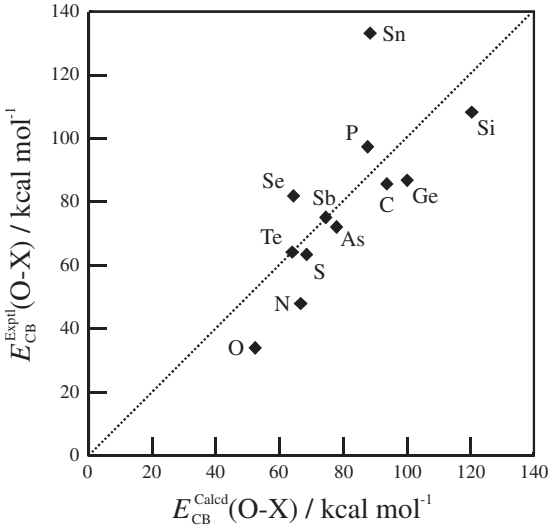

Figure 2. Comparison between calculated and experimental O–X covalent bond energies, E_{CB}^{Calcd}(O–X) and E_{CB}^{Exptl}(O–X) (in kcal mol^{-1}).

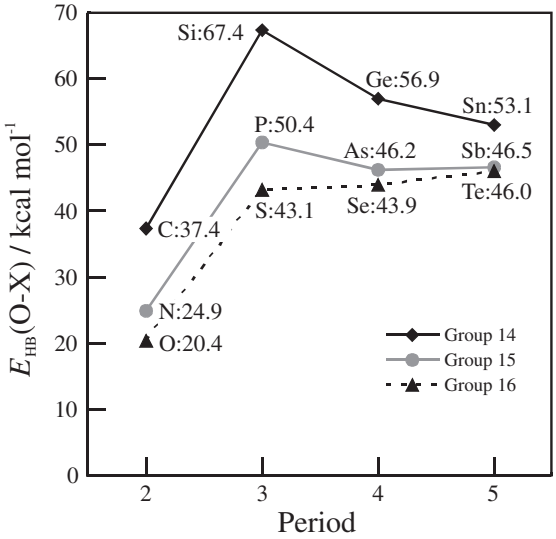

Figure 3. O–X hypervalent bond energies, E_{HB}(O–X) (in kcal mol^{-1}) with respect to group and period of X.

The energy of species of B′(α) and B″(α) should certainly be affected by steric and conjugation effects according to the structure. However, it was clarified that ΔE(B′) and ΔE(B″) are sufficiently close to each other. The maximum difference is at most 3.8 kcal mol^{-1} for [**8′**: Sn]. This fact supports the reliability of eq 1.

In Table 2, the experimental values for the O–X covalent bond energies,[21] E_{CB}(O–X), are also tabulated in parentheses. Note that the experimental value for **8′** corresponds to the Sn(II) ionic case. Figure 2 plots the comparison between the theoretical and experimental values for E_{CB}(O–X). Except for **8′** [Sn], there is a reasonable correspondence.

Figure 3 plots the estimated hypervalent bond energies, E_{HB}(O–X), with respect to period of the central atom. In all cases of groups 14–16, E_{HB}(O–X) for period 2 elements are remarkably smaller than the others. The weak interactions for period 2 elements are presumed to be the reason why B_{sym} structures of **5′**, **9′**, and **13′** become TSs. It is interesting that the order of E_{HB}(O–X) is groups 14 > 15 > 16 in each period. This tendency may be a result of the electronegativity of the central atom. The formal polarization of the hypervalent bond is described by $L^{-0.5}$–$X^{+1.0}$–$L^{-0.5}$. In consequence, the susceptibility to cation for the central atom determines the magnitude of the hypervalent bond. We examined the Kohn–Sham orbitals of the intermediates B_{sym}, and found the bonding, non-bonding, and anti-bonding orbitals for each compound which demonstrate the existence of hypervalent bond. The MOs are presented in Supporting Information.

N–X–N Hypervalent Bonds. This subsection deals with the N–X–N hypervalent bonds in **5**–**16**. Figure 4 shows the geometries of B_{sym} of **5**–**16** in Scheme 3. The species B_{sym} of central atoms of 14, 15, and 16 elements had C_{2v}, C_s, and C_{2v} symmetries, respectively, except for **13**-B_{sym} which had C_2 symmetry. The compounds with the central atoms X1 of period 3–5 elements were obtained as stable structures, whereas those of period 2 elements as TSs: i.e., **5**-B_{sym}, **9**-B_{sym}, and **13**-B_{sym}. The behaviors of the C5–X1 and X1–N2/X1–N8 lengths in **5**–**16** are similar to those of the C5–X1 and X1–O2/X1–O8 lengths in **5′**–**16′**. It should be noted that the X1–N2/X1–N8 lengths in **5**–**16** are slightly longer than the corresponding X1–O2/X1–O8 lengths, except for **13** and **13′**.

We estimated bond energies of the hypervalent N–X–N bonds in B_{sym} of **5**–**16** by the same procedure as described in the above subsection. Two processes shown in Scheme 6 were first investigated and the energy differences ΔE(B′) and ΔE(B″) were evaluated. From the dissociations of the N–X bonds in HNXH, the covalent bond energies E_{CB}(N–X) were estimated as follows:

$$E_{CB}(\text{N–X}) \approx E(\text{HN}\bullet) + E(\bullet\text{XH}) - E(\text{HNXH}) \quad (5)$$

By using E_{CB}(N–X) and the average of ΔE(B′) and ΔE(B″), namely $\overline{\Delta E}$, the N–X–N hypervalent bond energies were estimated:

$$E_{HB}(\text{N–X–N}) = E_{CB}(\text{N–X}) + \overline{\Delta E} \quad (6)$$

$$E_{HB}(\text{N–X}) = \frac{1}{2}(E_{CB}(\text{N–X}) + \overline{\Delta E}) \quad (7)$$

Table 3 compares the N–X bond lengths in B′, B″, and HNXH. The deviations from the HNXH case, which are shown in parentheses in Table 3, are less than 0.033 Å. This confirms the reliability of the covalent bond energy in eq 5 for the estimation of the hypervalent bond in B_{sym}.

Table 4 shows ΔE(B′), ΔE(B″), $\overline{\Delta E}$, E_{CB}(N–X), E_{HB}(N–X–N), and E_{HB}(N–X), for **5**–**16**. It was clarified that ΔE(B′) and ΔE(B″) are sufficiently close to each other. The maximum difference is 3.4 kcal mol^{-1} for [**8**: Sn]. This fact also supports the reliability of the average value $\overline{\Delta E}$.

Figure 5 plots the estimated hypervalent bond energies, E_{HB}(N–X). The behaviors of E_{HB}(N–X) are similar to those of E_{HB}(O–X) in Figure 3, i.e., those for period 2 elements are remarkably smaller than the others and the strength of the hypervalent bond is in the order of groups 14 > 15 > 16 in each period. It should be noted that E_{HB}(N–X) in Figure 5 are smaller than the corresponding E_{HB}(O–X) in Figure 3. This

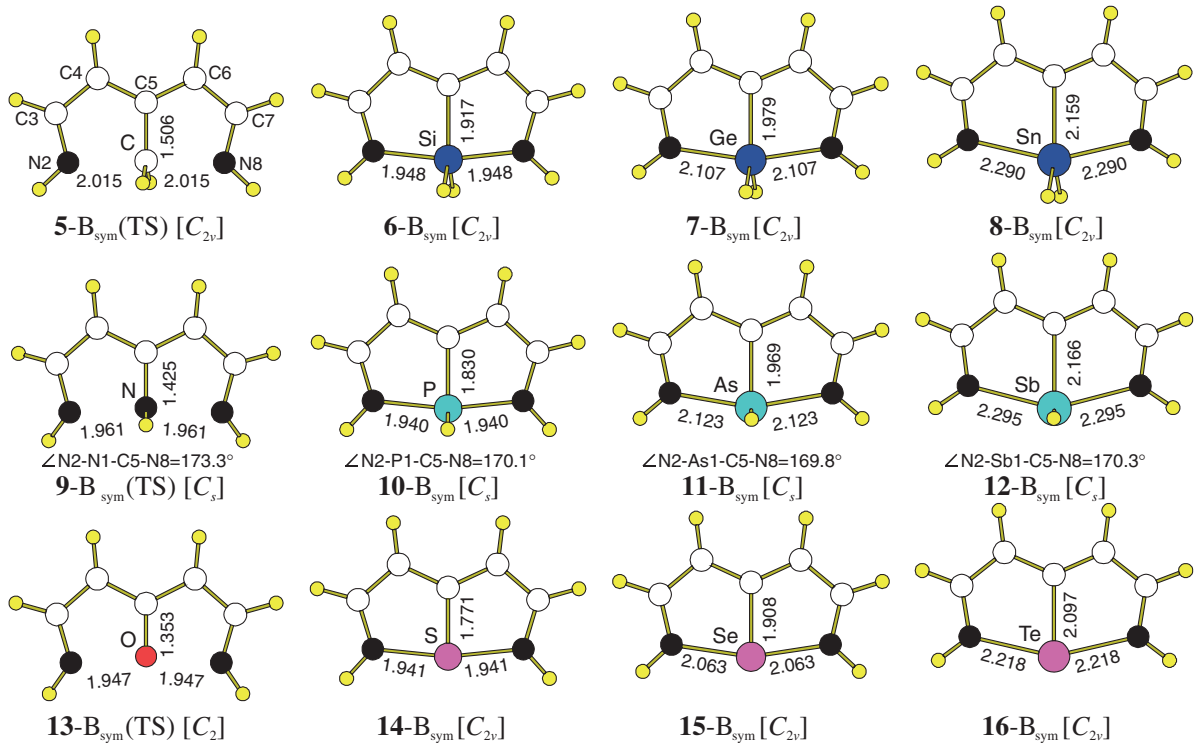

Figure 4. Geometries for B_{sym} of **5–16** (in Å).

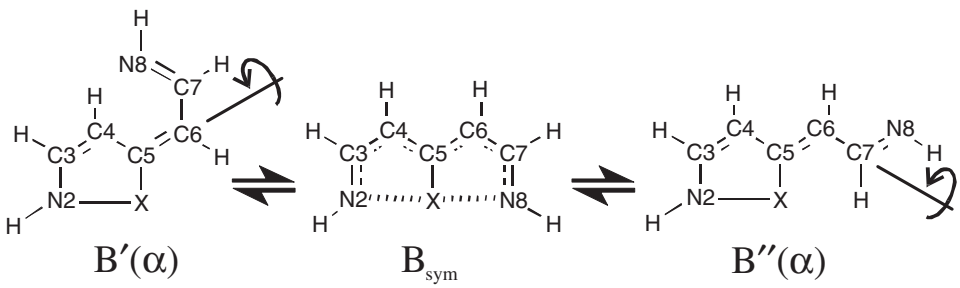

Scheme 6. Rotations of C5–C6 and C6–C7 bonds of **5–16** systems.

Table 3. N–X Bond Length in HNXH and **5–16** (in Å)[a)]

	5	**6**	**7**	**8**	**9**	**10**	**11**	**12**	**13**	**14**	**15**	**16**
X	CH_2	SiH_2	GeH_2	SnH_2	NH	PH	AsH	SbH	O	S	Se	Te
Group	14	14	14	14	15	15	15	15	16	16	16	16
Period	2	3	4	5	2	3	4	5	2	3	4	5
HNXH	1.464	1.732	1.854	2.055	1.436	1.721	1.871	2.064	1.447	1.734	1.880	2.049
B′	1.470	1.762	1.876	2.080	1.424	1.753	1.891	2.079	1.426	1.735	1.878	2.062
	(0.006)	(0.030)	(0.022)	(0.025)	(−0.012)	(0.032)	(0.020)	(0.015)	(−0.021)	(0.001)	(−0.002)	(0.013)
B″	1.473	1.762	1.877	2.082	1.432	1.754	1.895	2.083	1.433	1.745	1.889	2.073
	(0.009)	(0.030)	(0.023)	(0.027)	(−0.004)	(0.033)	(0.024)	(0.019)	(−0.014)	(0.011)	(0.009)	(0.024)

a) The deviations from the HNXH case are shown in parentheses.

tendency is also affected by the electronegativity of the atoms of positions 2 and 8 because of the formal polarization of the hypervalent bond, $L^{-0.5}$–$X^{+1.0}$–$L^{-0.5}$.

N–X···N Bond-Switching Equilibration. We here investigate the bond-switching equilibration of compounds **5–16** shown in Scheme 3. Our previous study,[9] which examined the reaction mechanism of **13** and **14** in detail, clarified that the stability of the symmetric intermediate B_{sym} determines the possibility of the bond-switching reaction. Figure 6 shows the geometries of the reactant A(α), which are equivalent to those of the corresponding products A(β). The frequency analyses confirmed that all species A(α) are stable structures. Both N2–X1 and C5–X1 lengths increase as higher period elements within the same group. The reversals for the N2–X1 lengths

Table 4. Energetic Results for **5**–**16** (in kcal mol^{-1})

	5	**6**	**7**	**8**	**9**	**10**	**11**	**12**	**13**	**14**	**15**	**16**
X	CH_2	SiH_2	GeH_2	SnH_2	NH	PH	AsH	SbH	O	S	Se	Te
Group	14	14	14	14	15	15	15	15	16	16	16	16
Period	2	3	4	5	2	3	4	5	2	3	4	5
$\Delta E(B')$	−33.91	16.61	13.69	19.49	−40.35	12.66	13.83	19.69	−43.13	11.50	20.08	29.08
$\Delta E(B'')$	−34.65	13.93	10.97	16.12	−39.47	11.19	11.99	17.05	−42.26	11.54	19.32	27.33
$\overline{\Delta E}$	−34.28	15.27	12.33	17.81	−39.91	11.93	12.91	18.37	−42.69	11.52	19.70	28.20
E_{CB}(N–X)	86.72	100.24	83.86	71.91	68.80	75.05	65.15	59.96	66.52	65.86	59.48	55.10
E_{HB}(N–X–N)	52.44	115.51	96.19	89.72	28.90	86.98	78.06	78.33	23.83	77.38	79.17	83.30
E_{HB}(N–X)	26.22	57.75	48.10	44.86	14.45	43.49	39.03	39.16	11.91	38.69	39.59	41.65

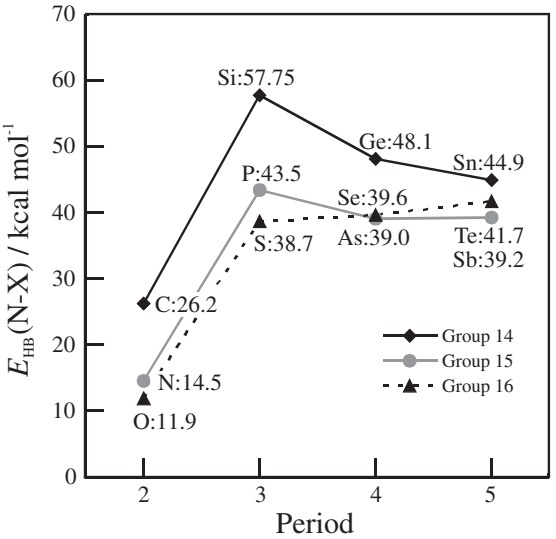

Figure 5. N–X hypervalent bond energies, E_{HB}(N–X) (in kcal mol^{-1}) with respect to group and period of X.

between periods 2 and 3 are not seen in this case. The other bonding characters are similar in all cases. For example, C3–C4 and C4–C5 lengths are 1.406–1.481 and 1.352–1.386 Å, which correspond to single- and double-bonds, respectively. From the geometrical point of view, no specific interactions between X1 and N2 appear in A(α) and A(β). Figure 6 also shows the relative energies of A(α) with respect to B_{sym}:

$$\Delta E(A) = E(A) - E(B_{sym}) \quad (8)$$

For **5**, **9**, **13**, and **14**, ΔE(A) become negative values. It means that the reactant A(α) as well as the product A(β) are more stable than the intermediate B_{sym} for the second period compounds. The opposite is true for the other compounds: **6**–**8**, **10**–**12**, **15**, and **16**.

Figure 7 plots ΔE(A) in eq 8 with respect to the period of the central atom X. In all cases of groups 14–16, ΔE(A) for period 2 elements are considerably smaller than the others. Furthermore, in each period, ΔE(A) increases in the order of groups 14 > 15 > 16. These behaviors resemble the hypervalent bond energies as described in Figure 5.

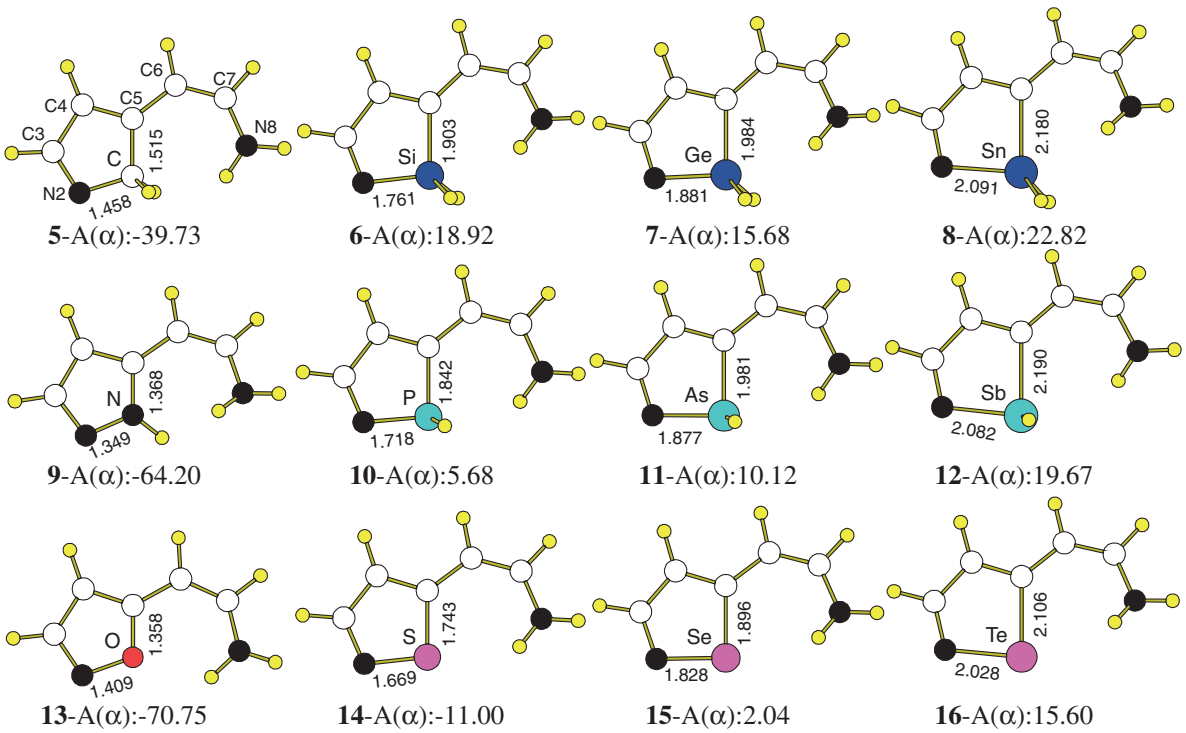

Figure 6. Geometries (in Å) and relative energies differences between A(α) and B_{sym} of **5**–**16**, ΔE(A) (in kcal mol^{-1}).

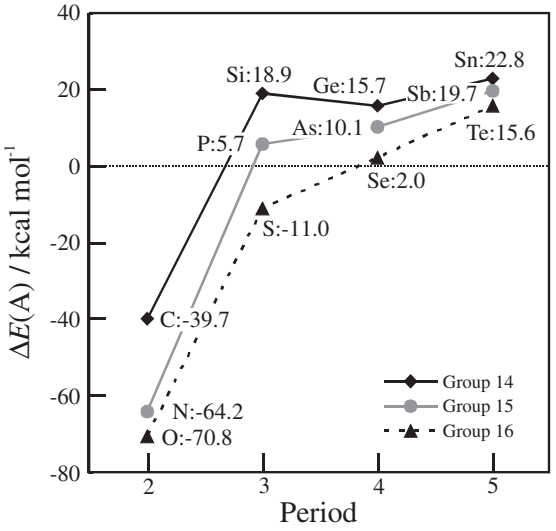

Figure 7. Energy difference between A and B_{sym}, ΔE(A) (in kcal mol^{-1}) with respect to group and period of X.

Conclusion

The hypervalent bond energies of O–X and N–X for symmetric species B_{sym} with central atoms X of group 14 [CH_2, SiH_2, GeH_2, SnH_2], 15 [NH, PH, AsH, SbH], and 16 [O, S, Se, Te] elements were estimated. It was clarified that B_{sym} for period 2 were obtained as TSs of which hypervalent bond energies were remarkably smaller than the others. Furthermore, the order of the hypervalent bond energies is groups 14 > 15 > 16 in each period. The O–X–O hypervalent bonds are stronger than the N–X–N bonds in all cases. These behaviors are a result of the electronegativities of the central atoms and the ligand atoms.

Part of the present calculations was performed at the Research Center for Computational Science (RCCS), Okazaki Research Facilities, and National Institutes of Natural Sciences (NINS). This study was supported in part by a Grant-in-Aid for Scientific Research on Priority Areas "Molecular Theory for Real Systems" KAKENHI 18066016 from the Ministry of Education, Culture, Sports, Science and Technology (MEXT), Japan; by the Nanoscience Program in the Next Generation Super Computing Project of the MEXT; by the Global Center Of Excellence (GCOE) "Practical Chemical Wisdom" from the MEXT; and by a project research grant for the "Development of high-performance computational environment for quantum chemical calculation and its assessment" from the Research Institute for Science and Engineering (RISE), Waseda University.

Supporting Information

Bonding, non-bonding, and anti-bonding orbitals of the intermediates B_{sym} which demonstrate the existence of hypervalent bond. This material is available free of charge on the web at http://www.csj.jp/journals/bcsj/.

References

1 K.-y. Akiba, T. Kobayashi, S. Arai, *J. Am. Chem. Soc.* **1979**, *101*, 5857.
2 F. Iwasaki, K.-y. Akiba, *Acta Crystallogr., Sect. B* **1981**, *37*, 185.
3 Y. Yamamoto, K.-y. Akiba, *J. Am. Chem. Soc.* **1984**, *106*, 2713.
4 Y. Yamamoto, K.-y. Akiba, *Bull. Chem. Soc. Jpn.* **1989**, *62*, 479.
5 K. Ohkata, Y. Ohyama, Y. Watanabe, K.-y. Akiba, *Tetrahedron Lett.* **1984**, *25*, 4561.
6 K.-y. Akiba, K. Kashiwagi, Y. Ohyama, Y. Yamamoto, K. Ohkata, *J. Am. Chem. Soc.* **1985**, *107*, 2721.
7 A. Hordvik, K. Julshamn, *Acta Chem. Scand.* **1972**, *26*, 343.
8 *Chemistry of Hypervalent Compounds*, ed. by K.-y. Akiba, Wiley-VCH, New York, **1999**.
9 T. Atsumi, T. Abe, K.-y. Akiba, H. Nakai, *Bull. Chem. Soc. Jpn.* **2010**, *83*, 520.
10 K. Ohkata, M. Ohsugi, K. Yamamoto, M. Ohsawa, K.-y. Akiba, *J. Am. Chem. Soc.* **1996**, *118*, 6355.
11 Y. Yamauchi, K.-y. Akiba, H. Nakai, *Chem. Lett.* **2007**, *36*, 1120.
12 A. D. Becke, *J. Chem. Phys.* **1993**, *98*, 5648.
13 J. C. Slater, *Phys. Rev.* **1951**, *81*, 385.
14 A. D. Becke, *Phys. Rev. A* **1988**, *38*, 3098.
15 S. H. Vosko, L. Wilk, M. Nusair, *Can. J. Phys.* **1980**, *58*, 1200.
16 C. Lee, W. Yang, R. G. Parr, *Phys. Rev. B* **1988**, *37*, 785.
17 T. H. Dunning, Jr., *J. Chem. Phys.* **1989**, *90*, 1007.
18 D. E. Woon, T. H. Dunning, Jr., *J. Chem. Phys.* **1993**, *98*, 1358.
19 K. A. Peterson, D. Figgen, E. Goll, H. Stoll, M. Dolg, *J. Chem. Phys.* **2003**, *119*, 11113.
20 M. J. Frisch, G. W. Trucks, H. B. Schlegel, G. E. Scuseria, M. A. Robb, J. R. Cheeseman, J. A. Montgomery, Jr., T. Vreven, K. N. Kudin, J. C. Burant, J. M. Millam, S. S. Iyengar, J. Tomasi, V. Barone, B. Mennucci, M. Cossi, G. Scalmani, N. Rega, G. A. Petersson, H. Nakatsuji, M. Hada, M. Ehara, K. Toyota, R. Fukuda, J. Hasegawa, M. Ishida, T. Nakajima, Y. Honda, O. Kitao, H. Nakai, M. Klene, X. Li, J. E. Knox, H. P. Hratchian, J. B. Cross, V. Bakken, C. Adamo, J. Jaramillo, R. Gomperts, R. E. Stratmann, O. Yazyev, A. J. Austin, R. Cammi, C. Pomelli, J. W. Ochterski, P. Y. Ayala, K. Morokuma, G. A. Voth, P. Salvador, J. J. Dannenberg, V. G. Zakrzewski, S. Dapprich, A. D. Daniels, M. C. Strain, O. Farkas, D. K. Malick, A. D. Rabuck, K. Raghavachari, J. B. Foresman, J. V. Ortiz, Q. Cui, A. G. Baboul, S. Clifford, J. Cioslowski, B. B. Stefanov, G. Liu, A. Liashenko, P. Piskorz, I. Komaromi, R. L. Martin, D. J. Fox, T. Keith, M. A. Al-Laham, C. Y. Peng, A. Nanayakkara, M. Challacombe, P. M. W. Gill, B. Johnson, W. Chen, M. W. Wong, C. Gonzalez, J. A. Pople, *Gaussian 03, Revision C.02*, Gaussian, Inc., Wallingford CT, **2004**.
21 *The Elements*, 3rd ed., ed. by J. Emsley, Oxford University, Oxford, **1998**.